N89-29874

5.2 WHY DO PLANETARY WAVE NUMBER ONE AND THE OZONE TRANSPORT VARY ANNUALLY IN THE NORTHERN HEMISPHERE AND SEMIANNUALLY IN THE SOUTHERN HEMISPHERE?

M. A. Geller, M. F. Wu

Code 610, NASA Goddard Space Flight Center
Greenbelt, MD 20771

E. R. Nash

Applied Research Corporation
Landover, MD 20785

Evidence is cited from our studies and those of others showing the different nature of the yearly variations of the middle atmospheres of the Northern and Southern Hemispheres. The Northern Hemisphere middle atmosphere is shown to be characterized by annual variations in planetary wave number one amplitude and the accompanying ozone transports. The Southern Hemisphere middle atmosphere is shown to be characterized by semiannual variations in the amplitude of planetary wave number one and the accompanying ozone transports. The amplitude of wave number two in both hemispheres appears to vary annually. Examination is made of the nature of the planetary wave forcing in both hemispheres as well as the planetary wave propagation characteristics in both hemispheres in an attempt to better understand this.

Storyline

(1) Both the O_3 and planetary wave activity show different behavior in the Northern and Southern Hemispheres. These changes are plausibly consistent with each other.
(2) Standing planetary wave number one shows an annual behavior in the Northern Hemisphere and a semiannual behavior in the Southern Hemisphere.
(3) Standing wave number two shows an annual behavior in both hemispheres.
(4) $\frac{dO_3}{dt}$ shows a semiannual behavior in the Southern Hemisphere and an annual behavior in the Northern Hemisphere. This indicates similar variations in the O_3 transports.
(5) Wave number one dominates the ozone transports in both hemispheres (more in the SH).
(6) The mean zonal wind in the lower troposphere displays an annual variation in the NH and a semiannual variation in the SH -- similar variations in the planetary wave forcings.
(7) The EP flux vectors show most vertical propagation in the NH winter and in the SH Fall and Spring. This is consistent with the theory of Charney and Drazin and the observed mean zonal winds.
(8) A recent model of Alan Plumb predicts that for small planetary wave forcing amplitudes (SH) the planetary waves behave linearly, consistent with the Charney-Drazin theory. For large forcing amplitudes (NH), the planetary waves decrease the mid-winter winds. This results in a semiannual planetary wave behavior in the SH and an annual behavior in the NH.
(9) An annual behavior in planetary wave 2 occurs at a lower forcing amplitude than is the case for planetary wave 1.

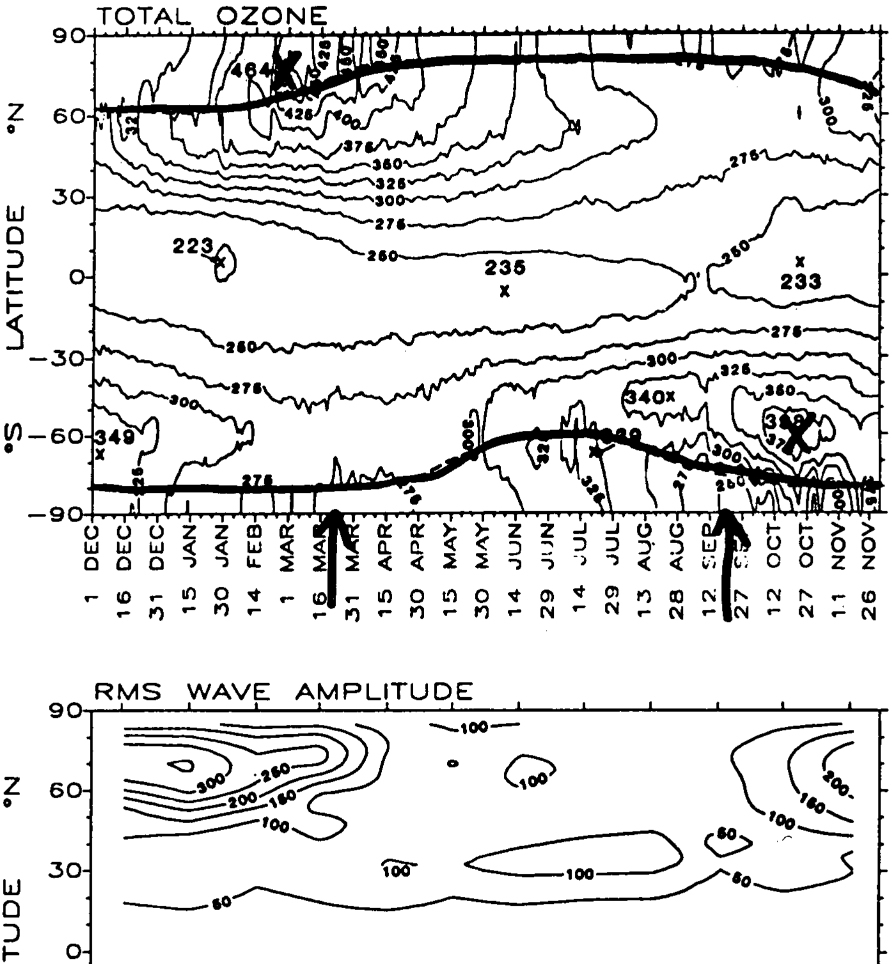

Figure 1. Top: Variation of SBUV-measured total ozone (in Dobson units) throughout the period December 1, 1978 to November 30, 1979. Bottom: Variation of the wave number one rms wave amplitude (in units of geopotential meters) at 100 mb for the period December to November [Geller and Wu, 1987].

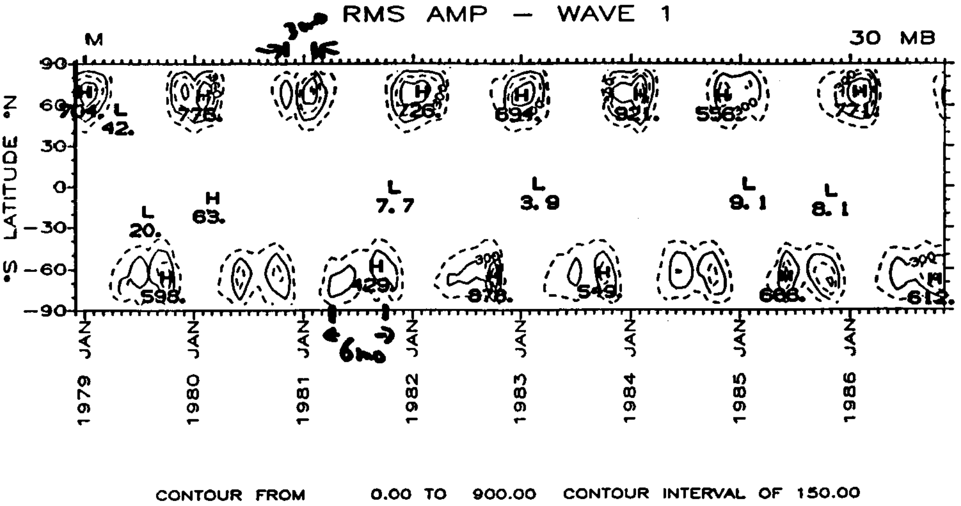

Figure 2. Variation of the wave number one rms wave amplitude (in units of geopotential meters) at 30 mb.

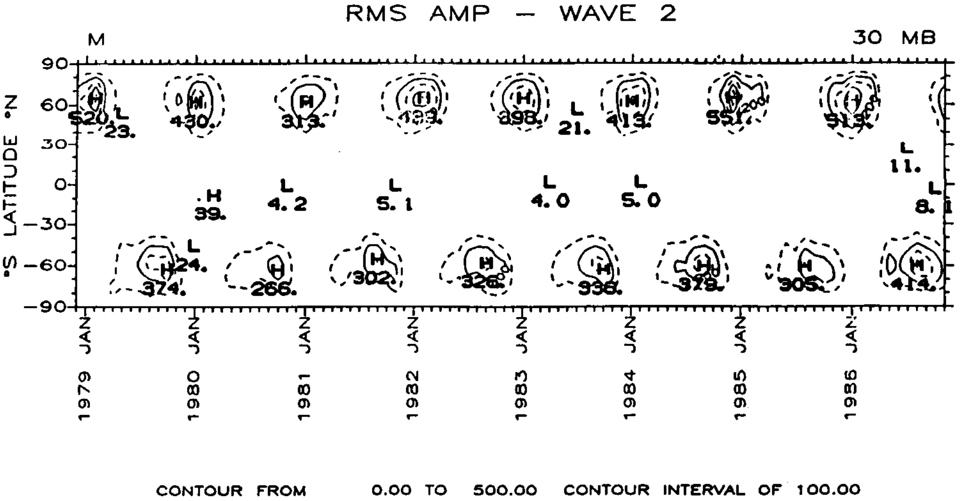

Figure 3. Variation of the wave number two rms wave amplitude (in units of geopotential meters at 30 mb.

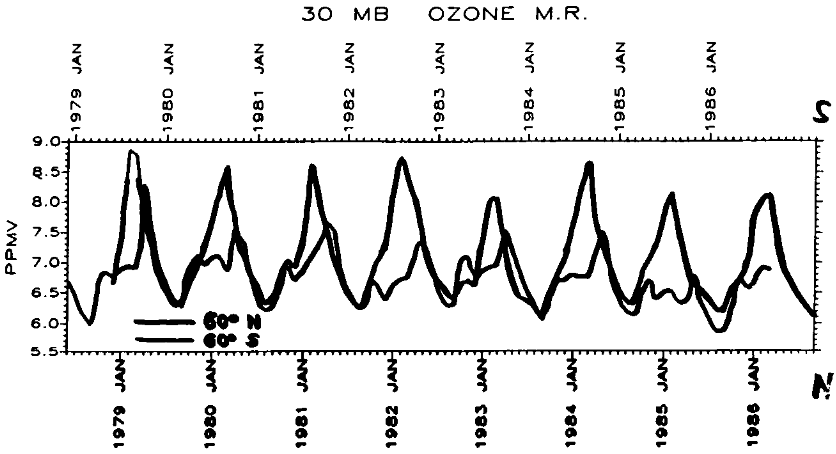

Figure 4. Variation of 30 mbar ozone mixing ratio (in ppmv) at 60°N and 60°S.

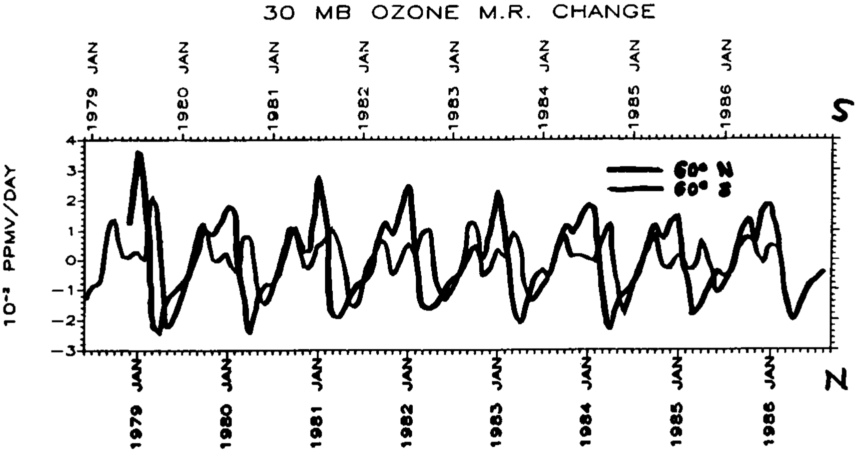

Figure 5. Variation of $\frac{dO_3}{dt}$ at 30 mbar in units of 10^{-2} ppmv/day at 60°N and 60°S.

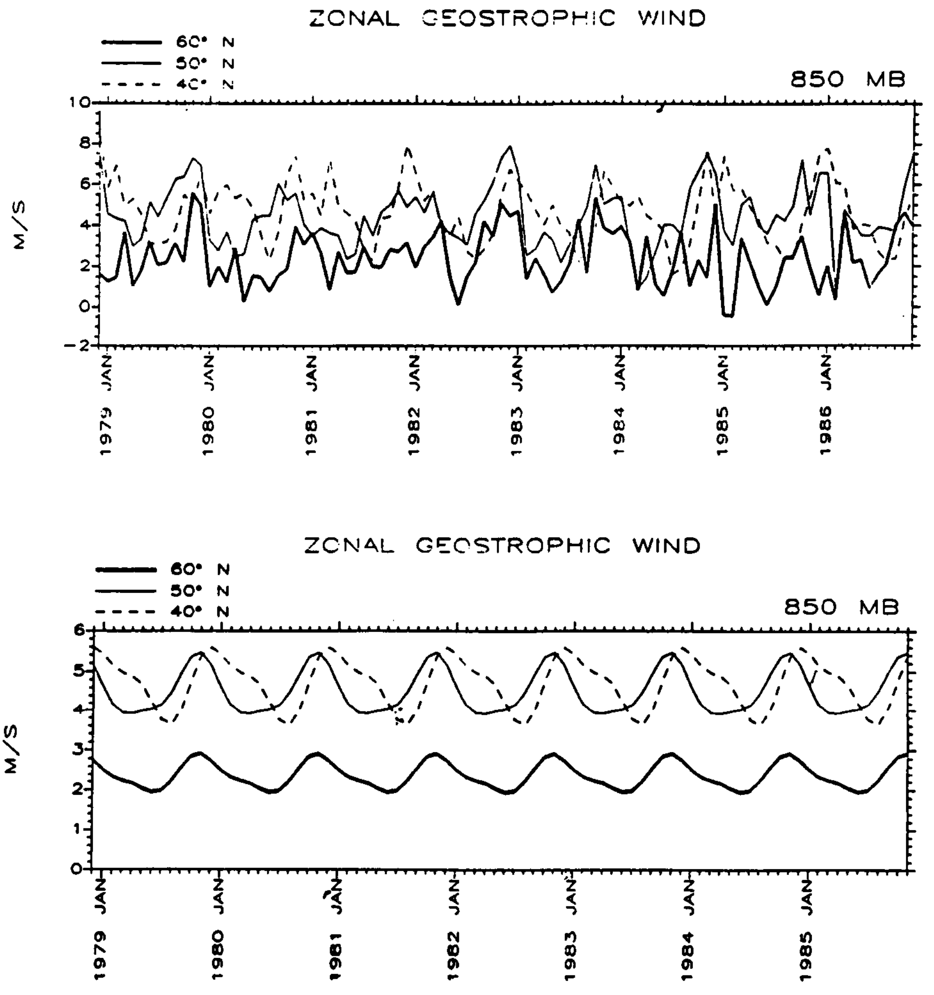

Figure 6. Mean zonal geospheric wind (in m s^{-1}) at 850 mb at 60°N, 50°N and 40°N. Top are monthly values and bottom is sum of annual and semiannual harmonics.

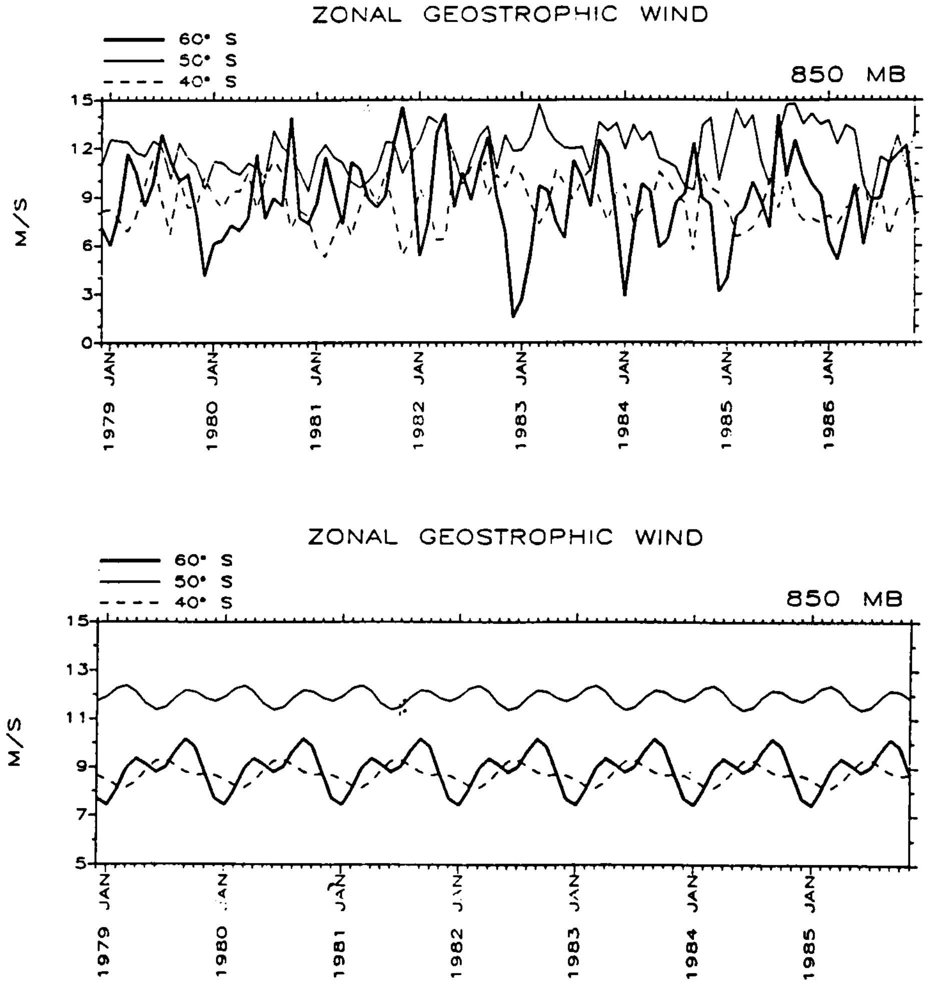

Figure 7. Mean zonal geospheric wind (in m s^{-1}) at 850 mb at 60°S, 50°S and 40°S. Top are monthly values and bottom is sum of annual and semiannual harmonics.

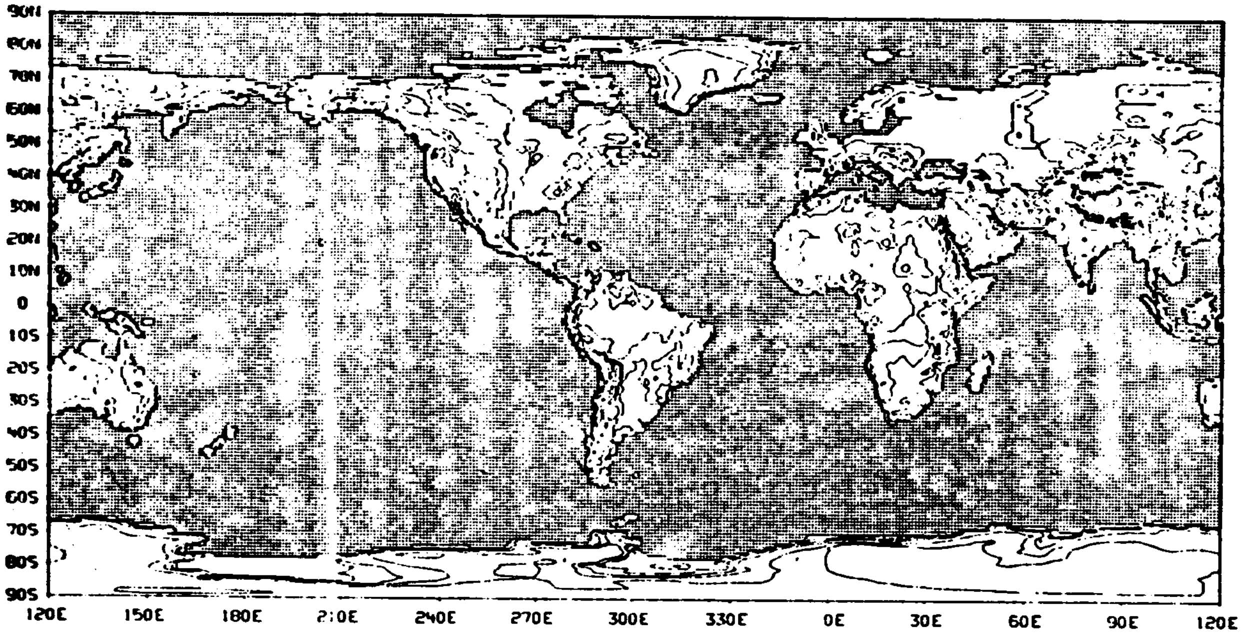

Figure 8. Analysis of the global terrain heights, with contours at 200, 500, 1000, 3000, 4000, 5000, 6000, 7000, 8000 m. The elevation of the coast is everywhere zero [Gates and Nelson, 1973].

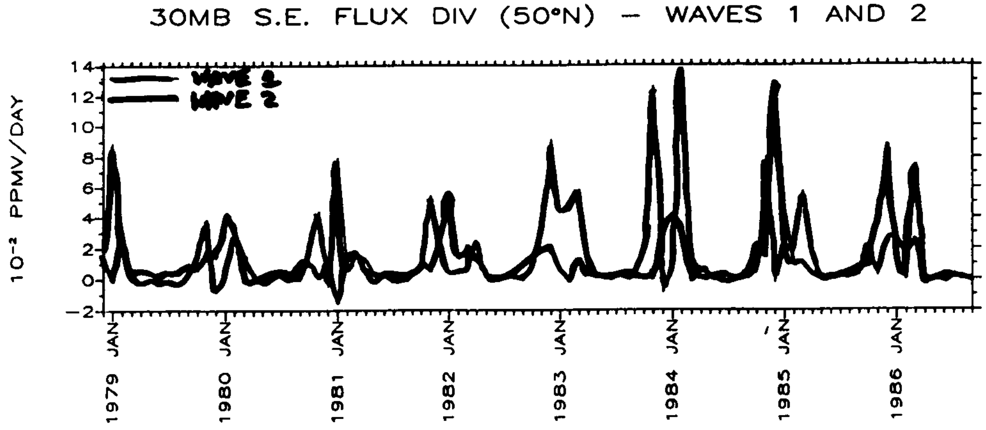

Figure 9. 30 mbar standing eddy divergence of O_3 flux at 50°N for wave numbers one and two.

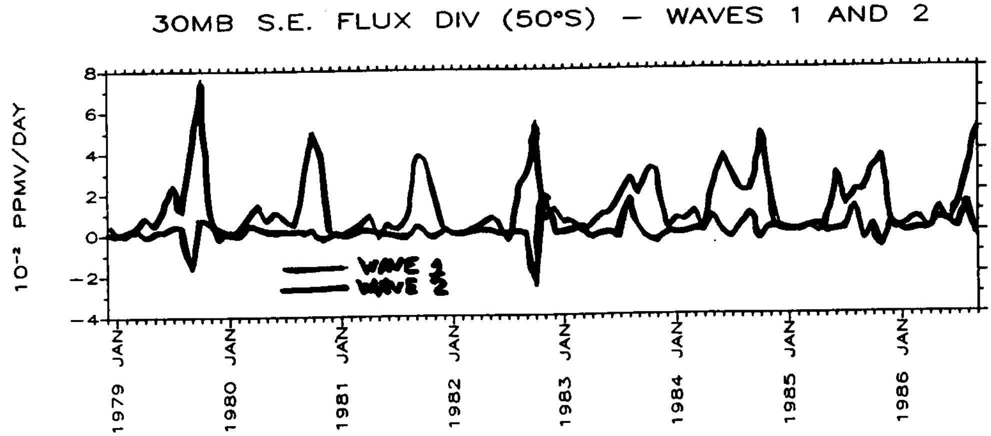

Figure 10. 30 mbar standing eddy divergence of O_3 flux at 50°S for wave numbers one and two.

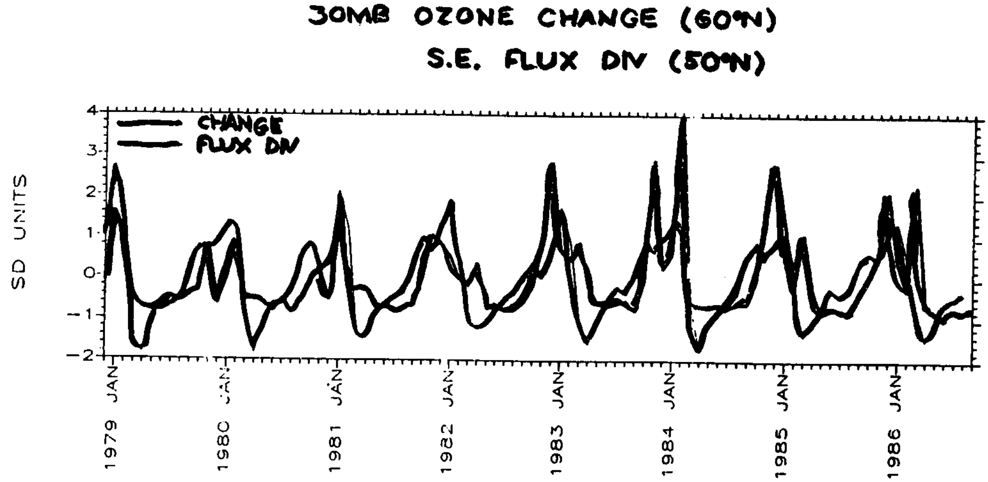

Figure 11. 30 mbar $\frac{dO_3}{dt}$ at 60°N and standing eddy ozone flux convergence at 50°N.

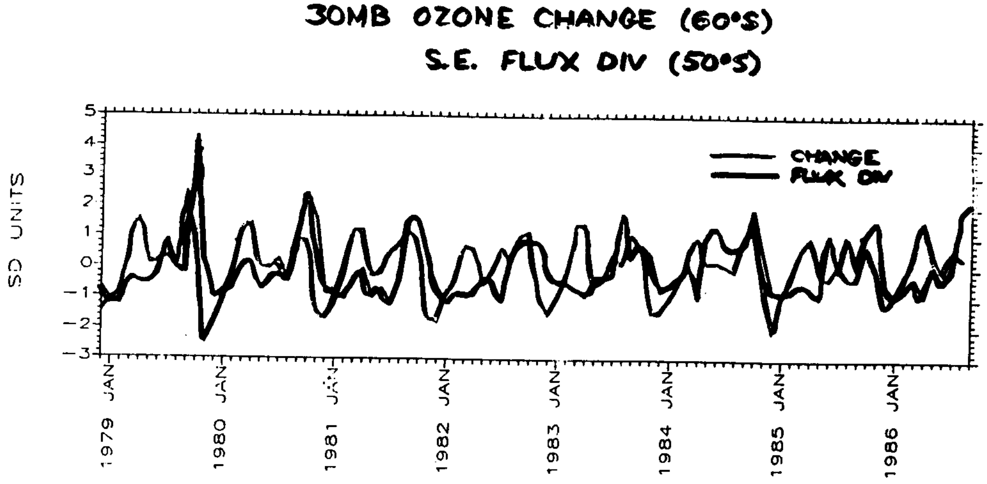

Figure 12. 30 mbar $\frac{dO_3}{dt}$ at 60°S and standing eddy ozone flux convergence at 50°S.

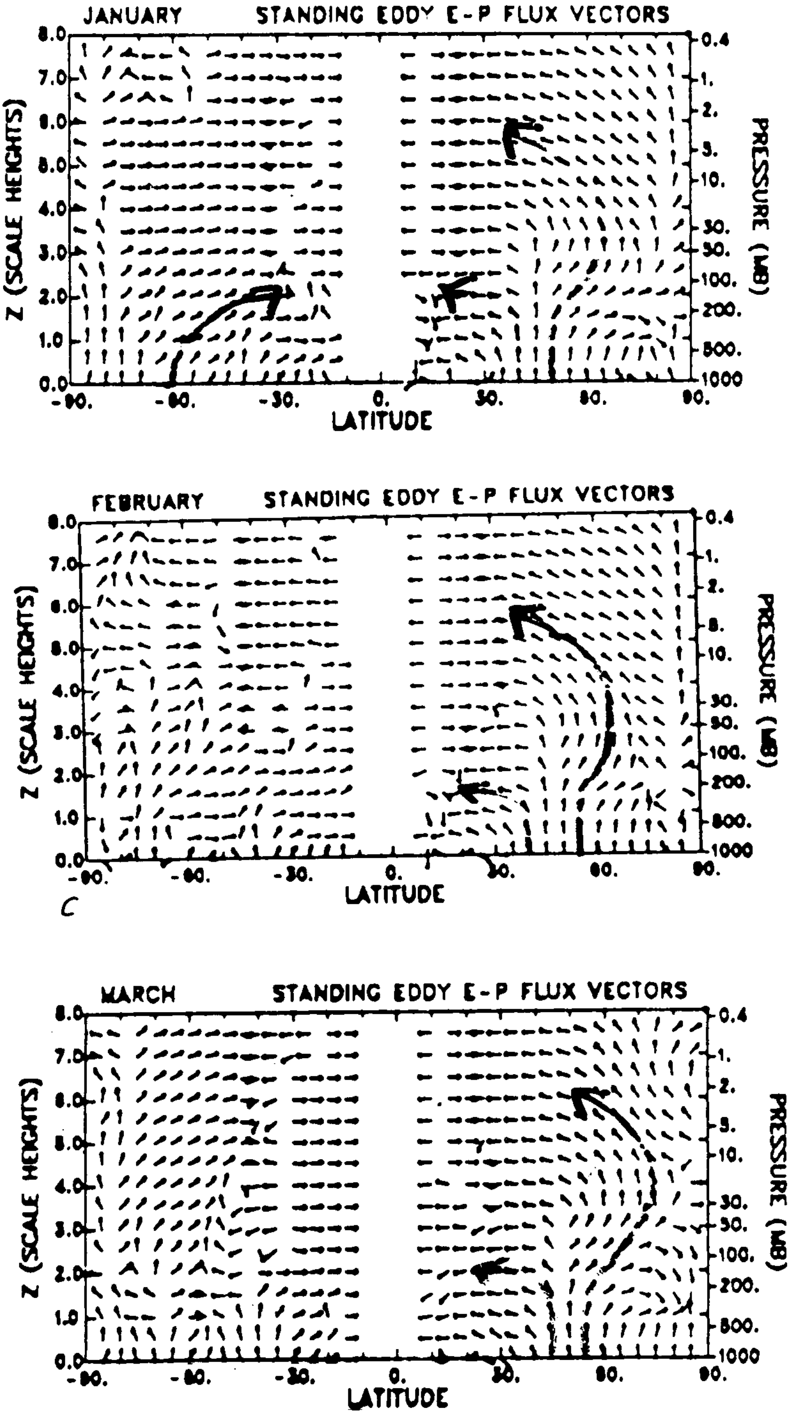

Figure 13. Monthly standing eddy Eliassen-Palm flux vectors (all the same length) for the 12 months.

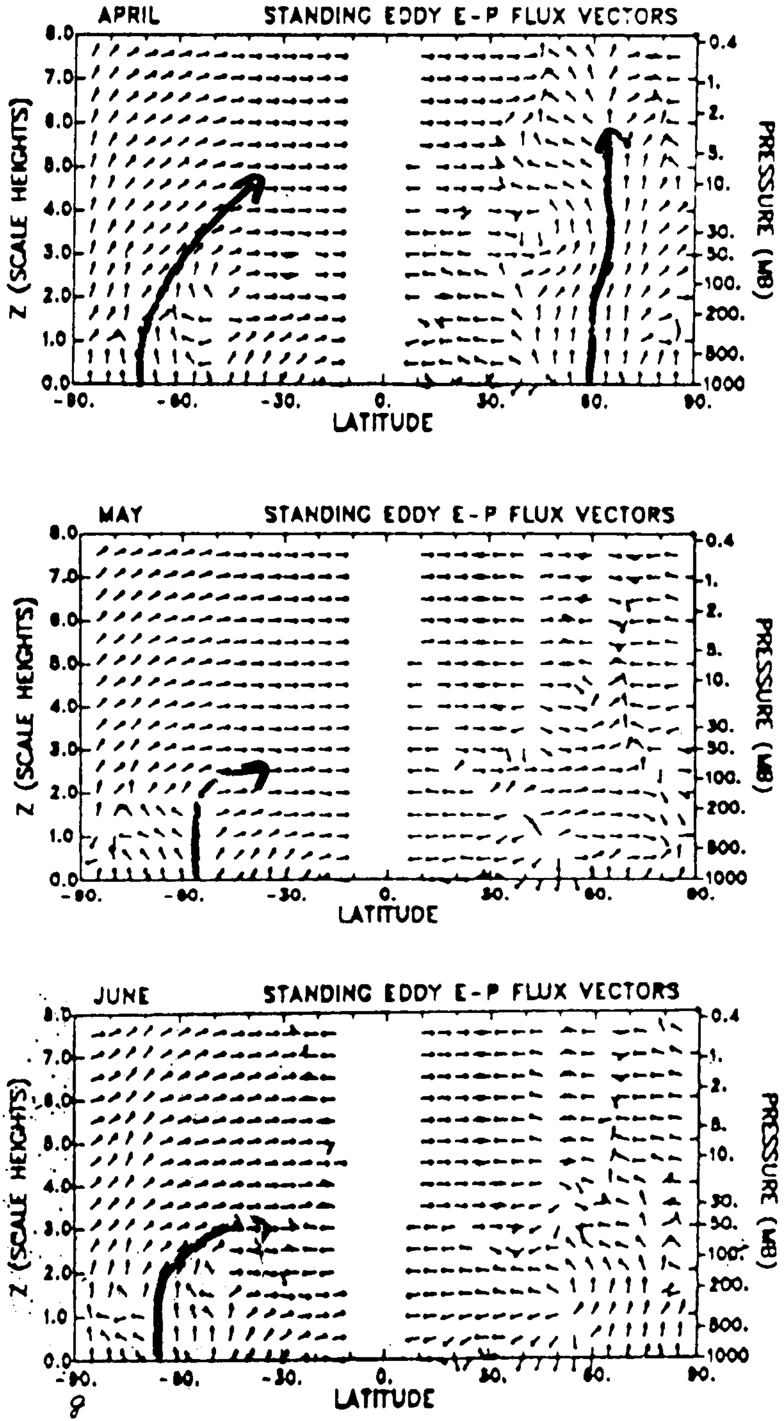

8

Figure 13 continued.

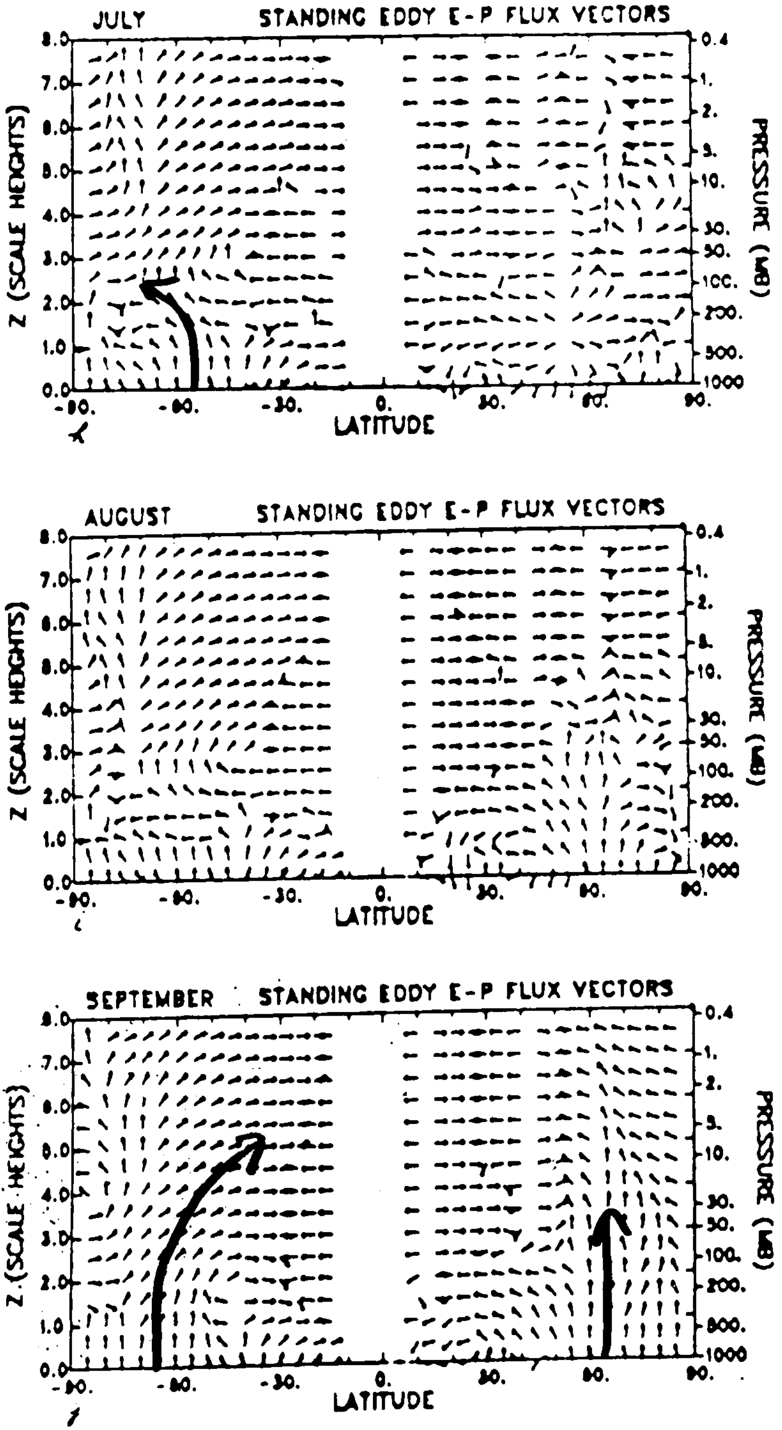

Figure 13 continued.

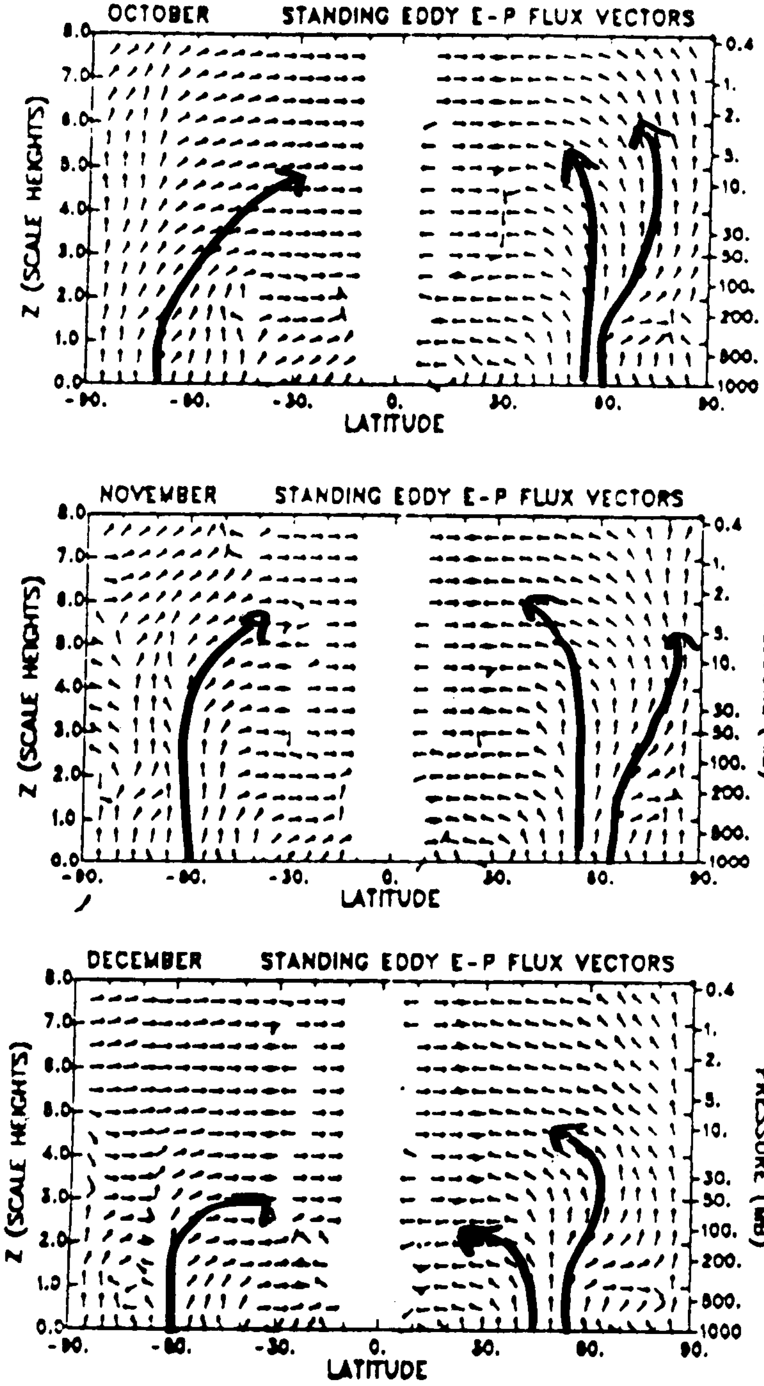

Figure 13 continued.

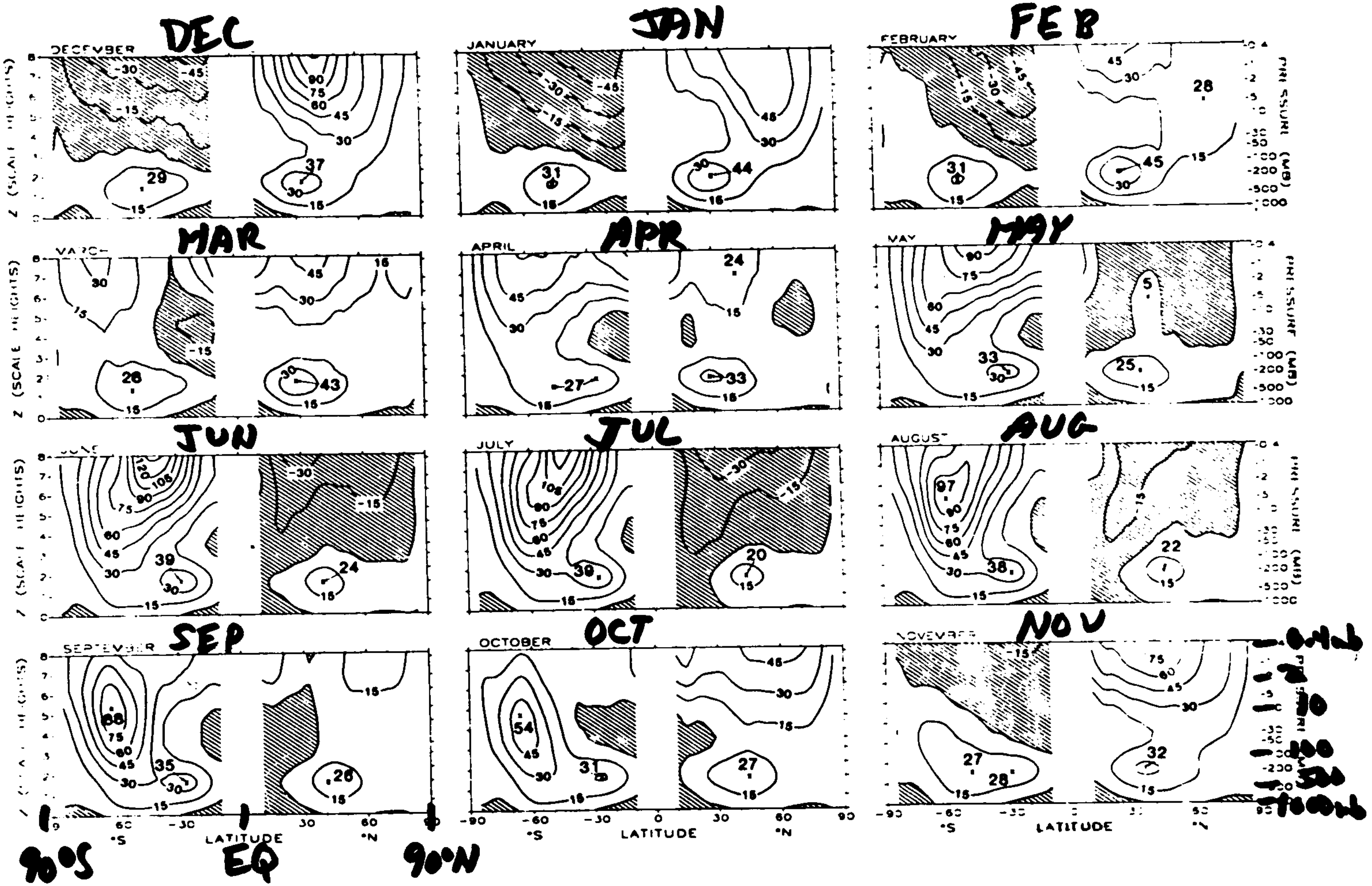

Figure 14. Monthly mean zonal winds (in m/s) for the 12 months of the year derived from a four-year data set.

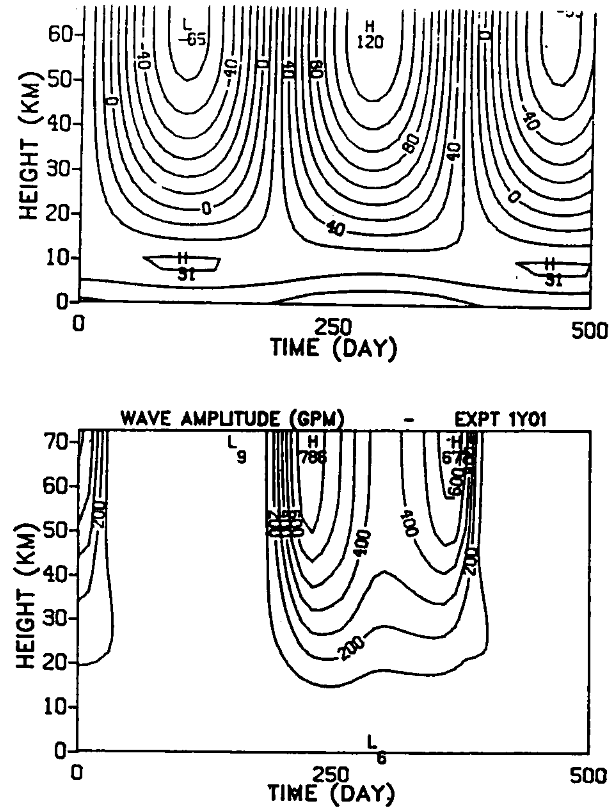

$[\bar{u}]$ ms^{-1}

wn 1

Labels x0.1

Figure 15. Top: Modeled mean zonal wind variation. Bottom: Modeled planetary wave number one amplitude. Result from Plumb (unpublished, 1988) for a forcing amplitude of 1 m at zero.

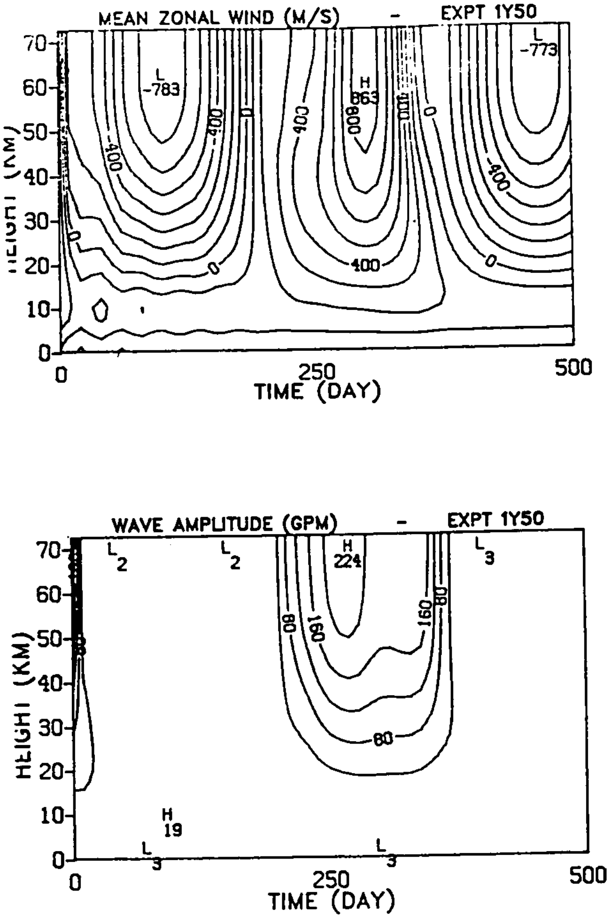

$[\bar{u}]\ \mathrm{ms}^{-1} \times 1$

wn 1

Figure 16. Top: Modeled mean zonal wind variation. Bottom: Modeled planetary wave number one amplitude. Result from Plumb (unpublished, 1988) for a forcing amplitude of 60 m at zero.

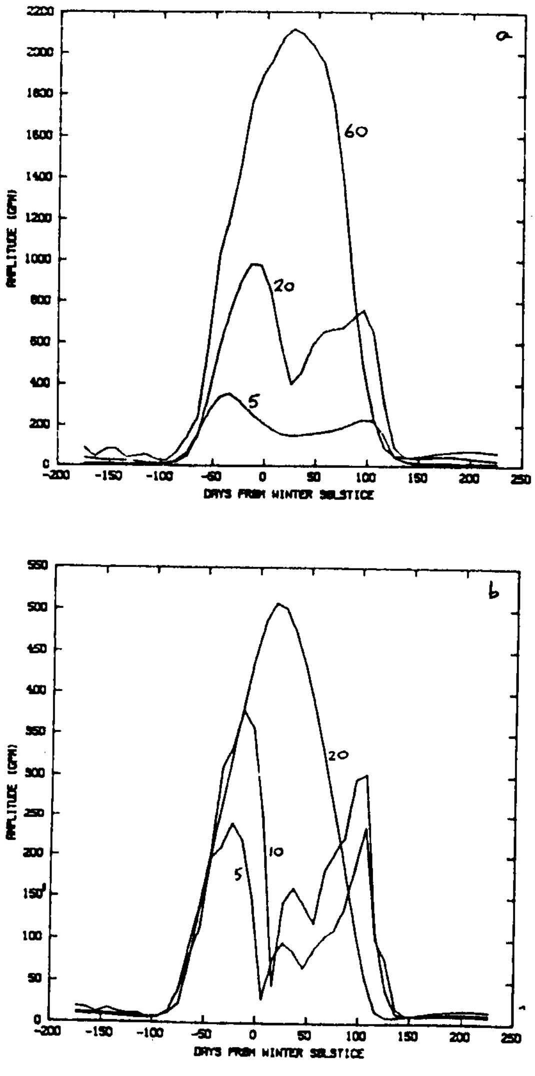

Figure 17. Response curves for wave number one (top) and wave number two (bottom) for different forcing amplitudes.

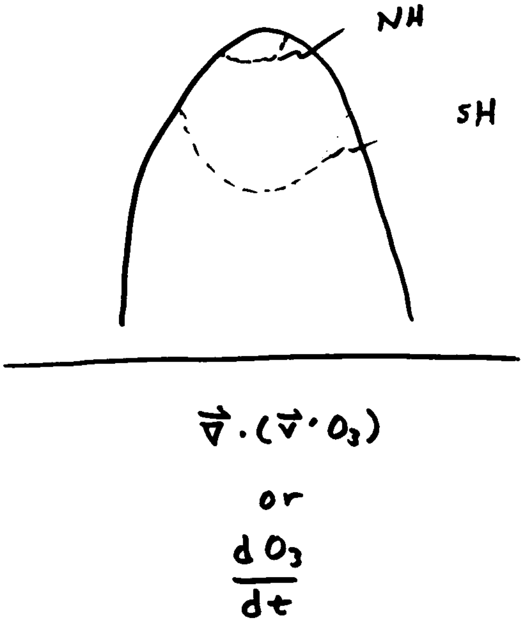

Figure 18. Schematic indicating large mid-winter notch out of ozone transport in the Southern Hemisphere and smaller one in the Northern Hemisphere.

Answer to our Original Question

It appears that the annual behavior of planetary wave one in the Northern Hemisphere and its semiannual behavior in the Southern Hemisphere are a result of the lower amplitude wave forcing in the Southern Hemisphere.

The annual cycle of the O_3 transports follow from this.